Minerals Engineering 203 (2023) 108325

Contents lists available at ScienceDirect

Minerals Engineering

journal homepage: www.elsevier.com/locate/mineng

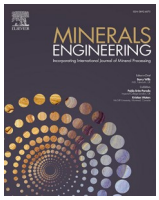

Alkaline pretreatment of a polymetallic sulfide (Fe-Pb-Mn) ore containing silver increases the efficiency of cyanidation by decreasing elemental sulfur content and by exposing sulfide surfaces

Gonzalo Larrabure [a,b], Dhamelyz Silva-Quiñones [c], Andrew V. Teplyakov [c], Juan Carlos F. Rodriguez-Reyes [a,b,*]

[a] Laboratory of Mineral and Ore Chemistry & Engineering – MOCHE, Universidad de Ingenieria & Tecnologia - UTEC, Jr. Medrano Silva 165, Lima 04, Peru
[b] Department of Chemical Engineering, Universidad de Ingenieria & Tecnologia - UTEC, Jr. Medrano Silva 165, Lima 04, Peru
[c] Department of Chemistry and Biochemistry, University of Delaware, Newark, DE 19716, USA

ARTICLE INFO

Keywords:
Leaching
Cyanide
Alkaline pretreatment
Polymetallic sulfide
Sulfur
XPS

ABSTRACT

Polymetallic sulfide ores are often not amenable to cyanide leaching due to the presence of several elements and minerals capable of interfering with this process. Thus, various strategies, such as chemical pretreatments, are often studied to improve the efficiency of cyanidation. Beyond the results of such strategies, it is important to understand the changes occurring on the mineral samples during these pretreatments. Herein, an alkaline pretreatment was applied to a silver concentrate (~8 kg Ag/t) composed of polymetallic sulfides (Fe-Pb-Mn), which increased the silver extraction during subsequent cyanidation from 40% to 80% and decreased the cyanide consumption in half (from approximately 60 to 30 kg NaCN/t). X-ray diffraction (XRD) and ICP-MS indicated that the pretreatment could remove significant amounts of elemental sulfur, which is a known cyanicidal agent. The dissolution of significant amounts of sulfur was confirmed by chemical analysis, which also demonstrated that the dissolution of iron, lead, manganese, and silver were negligible during pretreatment. At surface level, X-ray photoelectron spectroscopy (XPS) demonstrated that the pretreatment exposes fresh sulfide surfaces (e. g. pyrite). In addition, the XPS spectra indicated that the pretreatment facilitated the exposure of clean mineral surfaces. The presence of cleaner surfaces suggested a more uniform and less hindered diffusion of leaching agents through the mineral. Indeed, fitting the extraction data to the shrinking core model showed that pretreated samples featured a nearly ideal diffusion-controlled process, while in the case of untreated samples this fitting was less adequate. During cyanidation of both untreated and pretreated samples, lead build-up was detected on the surface (readsorption), which suggested that this phenomenon does not affect the efficiency of a leaching process. This study highlights the importance of combining bulk analytical methods with surface-sensitive techniques to obtain a more complete understanding of leaching processes.

1. Introduction

Leaching of both silver and gold is commonly performed using cyanide, as it forms thermodynamically stable compounds with these metals (Kyle, 1997; Lottermoser, 2003). Cyanidation is thus a well-known process, applied at large scale in various metallurgical plants around the world, despite its toxicity posing a threat to the environment and health. For simple silver species, such as metallic silver and silver sulfide, the underlying chemistry is known (Senanayake, 2008):

$$4Ag_{(s)} + 8CN^-_{(aq)} + O_{2_{(g)}} + 2H_2O_{(l)} \rightarrow 4Ag(CN)^-_{2(aq)} + 4OH^-_{(aq)} \quad (1)$$

$$Ag_2S_{(s)} + 4CN^-_{(aq)} + H_2O_{(l)} \rightarrow 2Ag(CN)^-_{2(aq)} + OH^-_{(aq)} + HS^-_{(aq)} \quad (2)$$

However, due to the continuous depletion of ore deposits that are amenable to cyanidation (Celep et al., 2019, 2011; Fleming, 1992), mines around the world yield ores with ever-growing complexity (Fraser et al., 1991; Khalid and Larachi, 2016). These complex ores can be referred to as refractory when they do not respond efficiently to standard metallurgical operations. For example, these ores may be composed of minerals which a) decrease the capacity of cyanide to dissolve target minerals or to diffuse through them (Birich et al., 2019; Jeffrey and

* Corresponding autor.
E-mail address: jcrodriguez@utec.edu.pe (J.C.F. Rodriguez-Reyes).

https://doi.org/10.1016/j.mineng.2023.108325
Received 4 May 2023; Received in revised form 9 August 2023; Accepted 12 August 2023
Available online 26 August 2023

Ritchie, 2000), b) lead to overconsumption of cyanide due the presence of sulfides or base metals in the ore (Bas et al., 2015; Portilla et al., 2020; Salas-Martell et al., 2020), and c) facilitate readsorption of leached precious metals on the surface of the ore (preg-robbing) (Larrabure and Rodríguez-Reyes, 2021; Senanayake, 2008; Tremolada et al., 2010). The first two effects are often responsible for the low efficiency in silver or gold extraction during the cyanidation of polymetallic sulfides. Despite that, cyanide leaching remains an attractive approach due to the relatively high content of precious metals in this type of ore (Arslan et al., 2003; Mikali et al., 2023).

Gold and silver are frequently embedded in a mineral matrix, so they are not located at the surface of ores, even after fine milling (Alarcón et al., 2018). As a result, it is necessary for cyanide (or any leaching agent) to diffuse through the mineral matrix to reach and dissolve the target metals. However, this is not always possible because certain matrixes prevent cyanide diffusion, limiting extraction to silver or gold particles with complete or partial liberation (Celep et al., 2009). Even in the case of a pervious mineral matrix, side reactions during cyanidation may create impermeable external layers which passivate the mineral particles (Khalid and Larachi, 2016; Silva-Quiñones et al., 2018). This is a common problem with sulfide and elemental sulfur-containing minerals (Zia et al., 2020, 2019), although it can occur in the presence of other minerals as well (Bas et al., 2018; Larrabure et al., 2021). In addition to the effects related to low cyanide diffusion, certain gold or silver-containing minerals are themselves insoluble or only partially soluble in the presence of cyanide in alkaline media. This is the case for silver-containing sulfosalts, such as tetrahedrite or tennantite (Celep et al., 2014), or of gold tellurides, such as calaverite (Aylmore, 2001).

While cyanide is the leaching agent of choice for gold and silver, it is known that the dissolution of these metals is not selective (Portilla et al., 2020). For example, cyanide will also form relatively stable compounds with copper, iron, cobalt, and nickel, if these base metals are present in the ore (Ciftci and Akcil, 2010; Dai et al., 2012; Jones and Hackl, 1999; Rees and Van Deventer, 2000). The occurrence of these side-reactions is detrimental towards the overall process because (1) it reduces the concentration of available cyanide, decreasing the expected kinetics of the leaching reaction, (2) it compromises the environmental and economic sustainability of cyanidation (Kianinia et al., 2018), and (3) the complexity of separation operations to extract gold and silver from leaching solutions will be greater due to the presence of other cyanide-metal compounds. In addition, other metals (e. g., copper) can catalyze the oxidation and decomposition of cyanide to species such as cyanate or thiocyanate. These reactions have a negative effect on leaching due to the loss of free cyanide in solution (Dai et al., 2012), (Kianinia et al., 2018).

Different pyrometallurgical or hydrometallurgical treatments have been studied in the past as feasible strategies to deal with ore refractoriness (Fleming, 1992; Fraser et al., 1991; La Brooy et al., 1994). Our group has mainly focused on the use of chemical pretreatments to make silver ores more amenable to cyanide leaching. Both acidic (sulfuric acid) (Portilla et al., 2020) and alkaline (sodium hydroxide) (Alarcón et al., 2018; Larrabure et al., 2021) pretreatments have been studied. The decision to use one of these two pretreatments depends both on the mineralogy of the ore and on the desired outcome. For example, an ore composed of copper and iron oxides and silver sulfides or sulfosalts was pretreated with an acidic solution, which removed most of the copper oxides that consumed cyanide during cyanidation. Even though the extraction of silver was only enhanced slightly, this pretreatment resulted in a significant decrease in cyanide consumption (Portilla et al., 2020). Similarly, the dissolution of copper and iron sulfides can be achieved by adding an oxidant (such as hydrogen peroxide) to a sulfuric acid solution (Salas-Martell et al., 2020).

In the case of polymetallic sulfides, however, it is apparent that an alkaline pretreatment is more efficient in terms of enhancing silver extraction, as observed in our studies of silver extraction from a polymetallic (Fe-Pb-Mn) sulfide ore (Alarcón et al., 2018; Larrabure et al., 2021). It was found that an alkaline pretreatment with sodium hydroxide can remove Mn species and expose fresh sulfide surfaces to the leaching solution, increasing silver extraction (from ~ 25% with conventional leaching to ~ 75% with cyanidation following the alkaline pretreatment). Although cyanide consumption was not affected by the pretreatment in this case, the alkaline pretreatment accelerated the initial kinetics for both silver extraction and cyanide consumption (Larrabure et al., 2021). Pre-oxidation treatments in alkaline media have also received attention as strategies to reduce cyanide consumption by oxidizing sulfide minerals. Both oxygen (Ellis and Senanayake, 2004) and hydrogen peroxide (Nunan et al., 2017) have been found to be effective at oxidizing sulfides before cyanidation of gold-containing ores, thus reducing cyanide consumption.

Characterization is key in investigating strategies to increase the efficiency of leaching processes. Commonly, sample characterization relies on polarization microscopy or electron spectroscopies, including the use of quantitative tools such as scanning electron microscopy – energy dispersive X-ray spectroscopy (SEM-EDX) or quantitative evaluation of minerals by scanning electron microscopy (QEMSCAN). While these techniques offer significant information, rationalizing changes at the topmost surface layers is the key to acquiring a complete understanding of the leaching process (Marabini et al., 1993). This is of particular importance when considering that the capacity of leaching agents to dissolve target metals relies heavily on their ability to diffuse through the ore, which could be hampered due to surface passivation (Senanayake, 2008; Silva-Quiñones et al., 2018). Thus, surface-level analysis techniques have been used in the past to achieve a greater understanding of both the kinetics and the thermodynamics of leaching operations and pretreatments (Graham and Bouwer, 2012; Larrabure et al., 2021; Marabini et al., 1993; Silva-Quiñones et al., 2018). Among the different techniques that are used to study the surfaces of samples, X-ray photoelectron spectroscopy (XPS) stands out as it can quantify the elements present at a surface-level and identify their oxidation states (De Caro et al., 2013; Godociková et al., 2002; Silva-Quiñones et al., 2018). Therefore, using XPS can provide key insight in processes such as surface passivation, preg-robbing, and enrichment or depletion of specific elements from the surface of minerals (De Caro et al., 2013; Deschênes et al., 2011, 2000; Graham and Bouwer, 2012; Hobson et al., 2006; Khoshkhoo et al., 2014; Parker et al., 2003; Yin et al., 2000). For example, previous research by our group has employed XPS to follow surface-level changes during sulfuric acid leaching of a copper-silver ore. The use of this technique demonstrated the reactivity of copper oxides in acid media, as opposed to copper and silver sulfides, which did not dissolve (Portilla et al., 2020). Our group has also combined polarization microscopy and XPS results to achieve a more thorough understanding of the cyanidation mechanism. Specifically, it was found that lead re-adsorption processes can occur during cyanide leaching of some complex ores (Silva-Quiñones et al., 2018). Another study by our group, in which hydrometallurgical and XPS results were combined, demonstrated that highly oxidized manganese-containing surface species can lead to passivation (Larrabure et al., 2021).

Herein, the strategy of combining hydrometallurgical results with surface-level analysis via XPS is employed to acquire a broader understanding of an alkaline pretreatment process and a subsequent cyanidation of a polymetallic sulfide.

2. Materials and methods

2.1. Samples and materials

The ore sample for this study was a silver-containing polymetallic sulfide obtained from a mining operation in the Peruvian Central Andes, which was milled to sizes below 150 μm (below mesh 100). The samples were characterized using X-ray diffraction analysis (*Bruker D2 Phaser* XRD) and inductively coupled plasma spectroscopy – mass spectrometry (*Spectro Arcos* ICP-MS). XRD analysis revealed that the main constituents

of the sample were galena, pyrite, and elemental sulfur, as displayed in detail in Table 1. A complete mineralogical distribution based on XRD analysis is presented in Supporting Information (Table S1). Additionally, ICP-MS indicated that the most abundant elements in the sample were sulfur, iron, manganese, and lead, as shown in Table 2. These characterization techniques were also employed to follow changes in the samples throughout experiments. Due to the low silver content in the ore, XRD was unable to identify silver-containing minerals. However, XPS determined that most of the silver present at the surface of the ore is in the form of silver sulfide. Similarly, XRD provided limited insight regarding the identity of manganese minerals, but XPS suggested that the surface of the ore contains oxidized species of Mn (III). Information based on XPS will be described in greater detail in the following sections.

2.2. Hydrometallurgical methods

The procedures for the alkaline pretreatment and the cyanide leaching tests presented in this section were adapted from validated methods used by our group (Alarcón et al., 2018; Portilla et al., 2020). Cyanide leaching experiments required mixing 200 mL of a NaCN solution (8 g/L) in an alkaline medium (pH 13) with 50 g of a mineral sample. The slurry (20% weight) was stirred mechanically (100 RPM) in a glass vase at ~ 20 °C during a period of 12 h. Free cyanide concentration and pH were monitored periodically throughout the experiments and controlled by adding more NaCN and NaOH if needed. Free cyanide concentration was determined by titrating 1 mL aliquots of leaching solution with silver nitrate (2 g/L), using rhodanine as an indicator. The pH of the leach solution was monitored with a pH-meter (Orion Star A324). Silver extraction during cyanidation experiments was calculated over the leaching period based on the concentration of silver in solution at various points in time. Silver concentration was determined by using atomic absorption spectroscopy (Perkin-Elmer® Atomic Absorption Spectroscopy 3110 model). Each cyanidation experiment was performed in triplicate.

The alkaline pretreatment with NaOH involved exposing the mineral samples to a NaOH solution (10 g NaOH/L) to yield a 25% solids slurry, which was kept at pH ~ 13 and 70 °C over a period of 4 h. The pH of the alkaline pretreatment was monitored periodically using pH 0–14 indicator strips (MColorpHast™). No additional NaOH was required during the pretreatments as the pH did not change. Each pretreatment was performed in triplicate. After the pretreatment, the solid residues were washed, filtered, and dried in an oven at 100 °C before subjecting them to cyanide leaching, following the procedure described previously. Similar to previous work from our group (Portilla et al., 2020), the ammount of oxygen dissolved during the experiments is considered negligible, as previous research has shown that open vessels, mechanically agitated through propellers, feature concentrations of dissolved oxygen below 1 ppm (Nunan et al., 2017).

The kinetics of leaching were studied considering the shrinking core model, which assumes functions for chemically-controlled and diffusion-controlled processes (Equations (3) and (4), respectively):

$$k_c.t = 1 - (1 - X)^{1/3} \quad (3)$$

Table 1
Bulk identification of main minerals by X-ray diffraction analysis in samples before and after performing an alkaline pretreatment with NaOH at pH ~ 13 and 70 °C for 4 h. A complete XRD analysis for the same samples is presented in Supporting Information (Table S1).

Mineral	Distribution before pretreatment (wt%)	Distribution after pretreatment (wt%)
Galena (PbS)	23.2	21.8
Pyrite (FeS_2)	22.5	23.8
Elemental sulfur (S_8)	8.9	–
Others	45.4	54.4

Table 2
Elemental analysis via ICP-MS of species of interest for as-received samples and pre-treated solid samples (before and after performing an alkaline pretreatment with NaOH at pH ~ 13 and 70 °C for 4 h), and the total extraction achieved for each species during the pretreatment based on solution assays. BLD: Element content below limit of detection during solution assays. OLD: Element content over limit of detection during solution assays.

Species content	As-received sample(wt%)	Pretreated sample(wt%)	Extraction of species during pretreatment (%, based on solution assays)
S	26.3	20.9	>3.8 (OLD)
Fe	13.3	15.2	<0.1 (BLD)
Mn	13.0	15.0	0.007 ± 0.001
Pb	21.7	22.3	0.003 ± 0.001
Ag	0.8	0.9	0.03 ± 0.01
As	1.0	1.1	0.9 ± 0.1
Sb	0.7	0.7	6.8 ± 0.9

$$k_d.t = 1 - 2X/3 - (1 - X)^{2/3} \quad (4)$$

where X is the molar fraction of silver leached and k_c and k_d are the rate constants for processes controlled chemically and by diffusion, respectively.

2.3. Characterization with XPS

Surface-level analysis of the ore samples was conducted on a Thermo Scientific K-Alpha + instrument equipped with an Al K-alpha source (hv = 1486.6 eV) at a 35.3° take-off angle. The base pressure during the measurements was $5x10^{-9}$ mbar. The survey spectra were collected over a binding energy range of 0–1000 eV with a pass energy of 100 eV, step size of 1 eV and dwell time of 10 ms. High resolution spectra of Fe 2p, Pb 4f, S 2p, Mn 2p, Ag 3d, C 1 s, and O 1 s regions were collected with a pass energy of 20 eV, step size of 0.1 eV, and dwell time of 50 ms. Sb 3d is presented together with O 1 s since their peaks overlap. The data was calibrated with C at 284.6 eV and processed with CasaXPS software (version 2.3.19) and Origin 2019.

The XPS spectral features were assigned based on previous research in our group (Larrabure et al., 2021; Portilla et al., 2020; Silva-Quiñones et al., 2018) and by others (Abdel-Samad and Watson, 1998; Ansari et al., 2019; Bastl and Baláz, 1993; Calderon et al., 2013; Carver et al., 1972; Derycke et al., 2013; Duan et al., 2018, 2017; Fantauzzi et al., 2015; Herbert et al., 1997; Kartio et al., 1997; Kaspar et al., 2010; Mills and Sullivan, 1983; Moulder et al., 1992; Oku and Hirokawa, 1976; Tiwari et al., 2018; Umezawa and Reilley, 1978; Wan et al., 2014). Table 3 summarizes the main peak assignments that are relevant for this study.

3. Results and discussion

3.1. Hydrometallurgical results

As shown in Fig. 1, cyanidation of the as-received ore led to an extraction of ~ 40% of total silver after 6 h of leaching (the reaction continued up to 12 h but the amount of silver leached did not change). Even though maximum silver extraction was achieved after 3 h, cyanide consumption continued increasing steadily, from 40 to 60 kg NaCN/t between the third and sixth hour of leaching. This is associated to the presence of other species reacting with cyanide, which should be removed from the sample before cyanidation to optimize cyanide consumption. On the other hand, performing an alkaline pretreatment with sodium hydroxide for 4 h increased silver extraction to ~ 80% after 6 h of cyanidation. The pretreatment also reduced cyanide consumption during leaching, which decreased to ~ 30 kg NaCN/t after 6 h. Thus, performing the alkaline pretreatment enhanced the leaching process, not only by increasing silver extraction but also by decreasing cyanide

Table 3
Characteristic peak assignment for Fe, Pb, S, Mn, and Ag species in XPS spectra.

Element (feature)	Assignment of peaks (eV)	Ref.
Fe (disulfide)	706.7–706.9	(Herbert Jr et al., 1997; Larrabure et al., 2021; Portilla et al., 2020; Silva-Quiñones et al., 2018)
Fe (other oxidized species)	710.8–711.4	(Derycke et al., 2013; Larrabure et al., 2021; Mills and Sullivan, 1983; Silva-Quiñones et al., 2018)
Pb (sulfide)	137.4	(Larrabure et al., 2021; Silva-Quiñones et al., 2018)
Pb (other oxidized species)	138.0–138.2	(Abdel-Samad and Watson, 1998; Bastl and Baláz, 1993; Larrabure et al., 2021; Silva-Quiñones et al., 2018)
S (elemental)	164.0–164.5	(Kartio et al., 1997; Moulder et al., 1992; Wan et al., 2014)
S (disulfides)	162.1–162.6	(Bastl and Baláz, 1993; Larrabure et al., 2021)
S (sulfate)	168.5–169.0	(Fantauzzi et al., 2015; Larrabure et al., 2021)
Mn (II) oxide	640.7–641.7	(Carver et al., 1972; Larrabure et al., 2021; Oku and Hirokawa, 1976)
Mn (III) oxide	641.8–642.4	(Carver et al., 1972; Larrabure et al., 2021; Umezawa and Reilley, 1978)
Mn (II) sulfide	640.4–640.5	(Carver et al., 1972; Larrabure et al., 2021; Tiwari et al., 2018)
Ag (metallic)	368.0–368.4	(Calderon et al., 2013; Duan et al., 2018, 2017; Kaspar et al., 2010)
Ag (dispersed species)	~369.4 (broad band)	(Calderon et al., 2013)
Ag (disulfide)	367.1	(Ansari et al., 2019)

consumption.

The kinetics of both conventional leaching and cyanidation after the alkaline pretreatment were also studied, following the shrinking core model (Eqns. (3) and (4). Fig. 2 shows that, in both cases, the cyanidation process can be better defined as a diffusion-controlled process. This implies that the kinetics of cyanide leaching with this ore is heavily dependent on the ability of cyanide to diffuse through the ore and for silver-cyanide complexes to diffuse towards the solution. As a result, the study of surface-level processes becomes fundamental, because the occurrence of such phenomena as passivation can severely limit the capacity of cyanide or oxygen to diffuse into the ore. It should be noted that the diffusion-controlled model fitted the data for the pretreated sample better ($R^2 = 0.98$) than the data for the untreated one ($R^2 = 0.91$). This suggests that the alkaline pretreatment removes species able to favor competing processes which may also be rate-limiting.

As mentioned above, the bulk changes in the mineralogy and in the elemental composition of the samples before and after performing the alkaline pretreatment are recorded in Table 1 and Table 2, with Table S1 (Supporting Information) providing a more complete mineralogical description. Table 1 suggests that, at a bulk-level, the main effect of the alkaline pretreatment was the removal of elemental sulfur. This is confirmed by analyzing the elemental composition of samples in Table 2, as sulfur is the only element whose concentration decreases during the alkaline pretreatment. This is likely due to the reaction of elemental sulfur that may yield soluble sulfides, polysulfides, and thiosulfates in the presence of hot sodium hydroxide solutions (Schweitzer and Pesterfield, 2010), which agrees with the information available from Pourbaix (potential vs. pH) diagrams (Anderson, 2016). The removal of elemental sulfur is noteworthy since it is a known refractory mineral that acts as a preg-robber, as a passivating agent, and as a cyanicidal mineral (Larrabure and Rodríguez-Reyes, 2021). The assays of the alkaline solution after pretreatment (Table 2) adds further insights about this process. These assays are consistent with other results discussed above: significant sulfur extraction was achieved during the pretreatment (over the detection limit for ICP-MS). Likewise, solution assays reveal that the pretreatment can also remove antimony and arsenic species to a certain extent. Even though the importance of

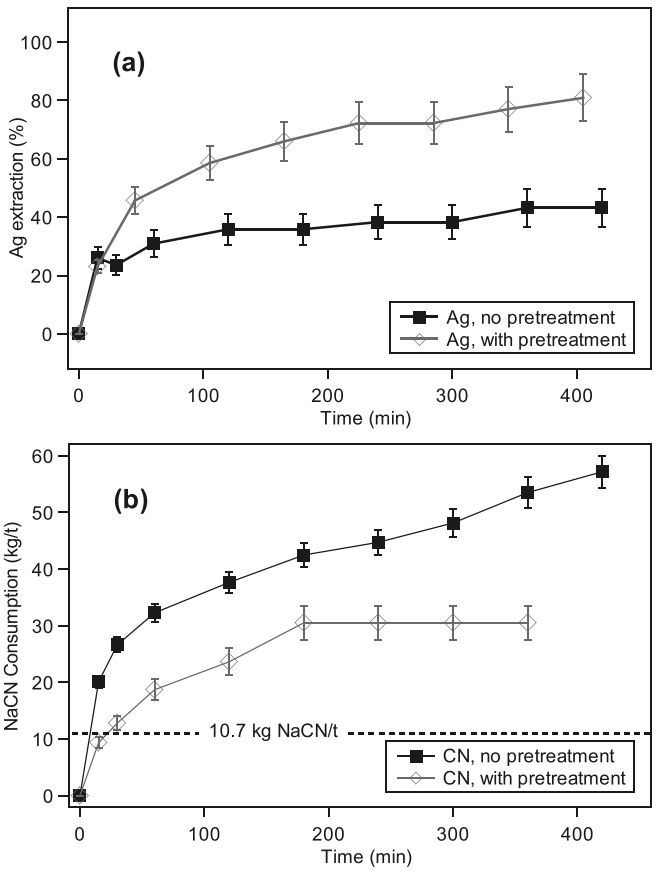

Fig. 1. (a) Silver extraction and (b) cyanide consumption during the leaching of a polymetallic (Fe-Pb-Mn) sulfide using conventional leaching and leaching after an alkaline pretreatment. The dotted line indicates the theoretical amount of cyanide needed to leach all the silver from the ore. Pretreatment conditions: 50 g of concentrate in 200 mL NaOH (10 g/L) at 80 °C for 4 h. Leaching conditions: 50 g of concentrate in 200 mL of NaCN (8 g/L) at 25 °C.

removing arsenic and antimony has been noted previously (Celep et al., 2014; Fraser et al., 1991; Larrabure and Rodríguez-Reyes, 2021), the removal of these elements is significantly lower in the present case and therefore this factor is not expected to be significant. Due to this, the identification of the minerals that contain arsenic and antimony is beyond the scope of this study. Importantly, silver extraction was not significant during the pretreatment: only 2.7 g Ag/t were removed, which accounts for ~ 0.03% of total silver. After elucidating noticeable changes based on the hydrometallurgical results, this study will now focus on assessing surface-level processes and how these may yield insights into the leaching process from a different perspective.

3.2. Surface-level analysis

In this section, a study of the surface-level processes that occur during cyanidation and during the alkaline pretreatment will be presented to complement the hydrometallurgical and mineralogical results presented above. Fig. 3 shows the XPS spectral regions of iron, lead, sulfur, silver, and manganese, which are the most informative elements found in the XPS survey. Additionally, the elemental surface-level composition changes of these elements are presented in Table 4, based on the study of the survey spectra of the mineral before, during, and after the pretreatment and cyanidation.

3.2.1. Surface-level analysis of conventional leaching

The surface-level elemental analysis presented in Table 4 reveals that both iron and silver content on the surface of the ore decrease slightly

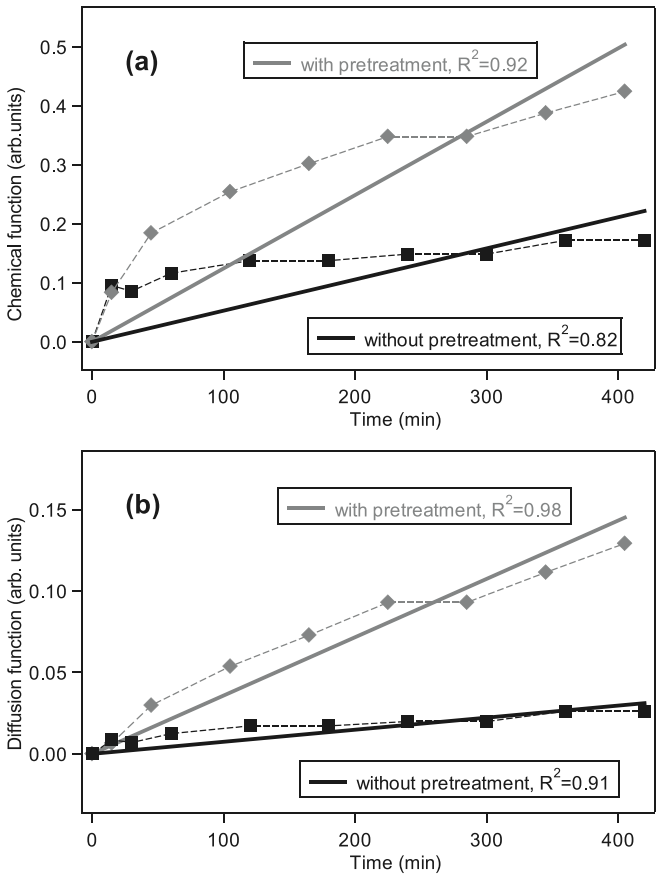

Fig. 2. Adjustment of the silver extraction data (Fig. 1) for both conventional leaching and leaching after performing an alkaline pretreatment to the shrinking core model. (a) Chemical reaction control function (Eqn. (3)); (b) diffusion control function (Eqn. (4)). The mechanism of cyanide consumption during the leaching of a polymetallic (Fe-Pb-Mn) sulfide was found to be diffusion-controlled.

during the first 2 h of cyanidation, although no further compositional changes are identified for these metals during the remaining cyanide leaching period. On the other hand, manganese surface-level content decreases steadily during the process. Sulfur content on the surface of the mineral increases significantly during the first 2 h of cyanide leaching, after which no further significant changes are identified. However, lead surface-level content continues increasing throughout the duration of the experiment.

Both iron disulfide (pyrite) and oxidized iron species can be identified in the iron spectral region in Fig. 3. Iron disulfide does not appear to change chemically during cyanidation, and the corresponding peak intensity remains constant. As a result, it is apparent that the pyrite present in the untreated ore is stable in the presence of cyanide in alkaline media. On the other hand, oxidized iron species seemingly undergo both reduction (peaks associated to oxidized iron species shifted, Fig. 3) and dissolution reactions (surface-level iron content decreased during first two hours, Table 4) during cyanidation. The dissolution of oxidized iron species is apparently associated with the alkaline conditions, since it can be identified both during conventional leaching (which is performed in alkaline conditions) and during the alkaline pretreatment. However, the reduction of oxidized iron species is only apparent during cyanidation.

The lead spectral region shown in Fig. 3 indicates that the untreated ore has both lead sulfide (galena) and oxidized species on the surface. However, the peaks corresponding to oxidized lead species increase in intensity during cyanidation, while lead sulfide peaks do not exhibit significant changes, although they are still distinguishable after cyanidation. Surface-level elemental composition changes (Table 4) reveal that lead content increases significantly throughout cyanide leaching, which can be explained by one of the following hypotheses: (1) cyanidation removes original surface-level species that do not contain lead, revealing lead species that were previously under the first few nanometers, or (2) lead species are being leached from within the ore by cyanide and are later re-adsorbed over the surface. Previous studies by our group have identified that the latter possibility is the most likely reason why the surface content of this metal increases during cyanidation of lead-containing polymetallic sulfides. These studies have also discussed the fact that lead re-adsorption does not seem to affect silver extraction efficiency (Larrabure et al., 2021; Silva-Quiñones et al., 2018). The hypothesis of lead re-adsorption agrees well with the possibility that the spectral signals of other elements may become less intense during cyanidation, because they are being covered under a layer of lead-containing species.

The sulfur region of the XPS spectra in Fig. 3 shows that the surface of the untreated sample is rich in both sulfides and oxidized sulfur species. These species seem to be cleaned-up during cyanidation, since the broad signals observed originally sharpen and increase in intensity. In particular, a small feature below 161 eV is detected as leaching progresses. This region can be associated with the presence of fresh layers of galena or pyrite, suggesting that fresh sulfide/disulfide surfaces are exposed during leaching. Further confirming this hypothesis, Table 4 shows that sulfur content was found to increase only during the first 2 h of leaching, which agrees with a scenario where an initial external layer covering the ore is dissolved by the leaching solution.

The manganese region of the spectra displayed in Fig. 3 indicates that the untreated ore is initially rich in Mn (III) oxidized species. However, some of these species undergo a reduction to Mn (II) which can be identified after 2 h of cyanide leaching. The manganese region of the spectra then remains unchanged during the rest of the cyanidation process. Nonetheless, the elemental concentration of surface-level manganese decreases throughout the leaching period (Table 4), which is likely associated with the removal of some cyanide-soluble manganese species. However, the decrease in the surface concentration of manganese can also be related to the re-adsorption of other elements (mainly lead) over the surface, blocking manganese detection by XPS.

The silver region of the XPS spectra shown in Fig. 3 reveals that the silver content of the untreated ore is mainly in the form of silver sulfide (Ag_2S), however metallic forms are also present as indicated by a broad feature around 370 eV. The intensity of all silver signals decreases during cyanide leaching: the surface concentration of silver (Table 4) exhibits a sharp decrease during the first 2 h of cyanidation, remaining constant during the rest of the cyanidation period. In addition to cyanidation of silver sulfide via Eqn. (2), the presence of lead in the leaching system suggests a second possible reaction for silver sulfide dissolution. The presence of Pb (II) in the reaction medium can render silver sulfide more amenable to cyanide leaching, according to Eqn. (5), which has an equilibrium constant of $10^{19.2}$ (Senanayake, 2008):

$$Ag_2S_{(s)} + 4CN^-_{(aq)} + Pb^{2+}_{(aq)} = 2Ag(CN)^-_{2(aq)} + PbS_{(s)} \quad (5)$$

In addition to these elements, oxygen (overlapped with antimony) and carbon spectral regions were followed (Fig. S1, Supporting Information section). The carbon spectral region initially shows a broad peak corresponding to carbonaceous and oxidized carbon species, which are removed from the surface during leaching. The O 1 s broad peak of the untreated ore confirms that there were originally multiple oxidized species (such as carbonates and hydroxides), which were also removed. Antimony is observed more clearly after leaching, which suggests that mineral species containing this element are exposed as leaching progresses.

3.2.1.1. Surface-level analysis of alkaline pretreatment and leaching. As discussed before based on Table 2, the alkaline pretreatment dissolves mainly sulfur-containing species. Other elements, such as iron,

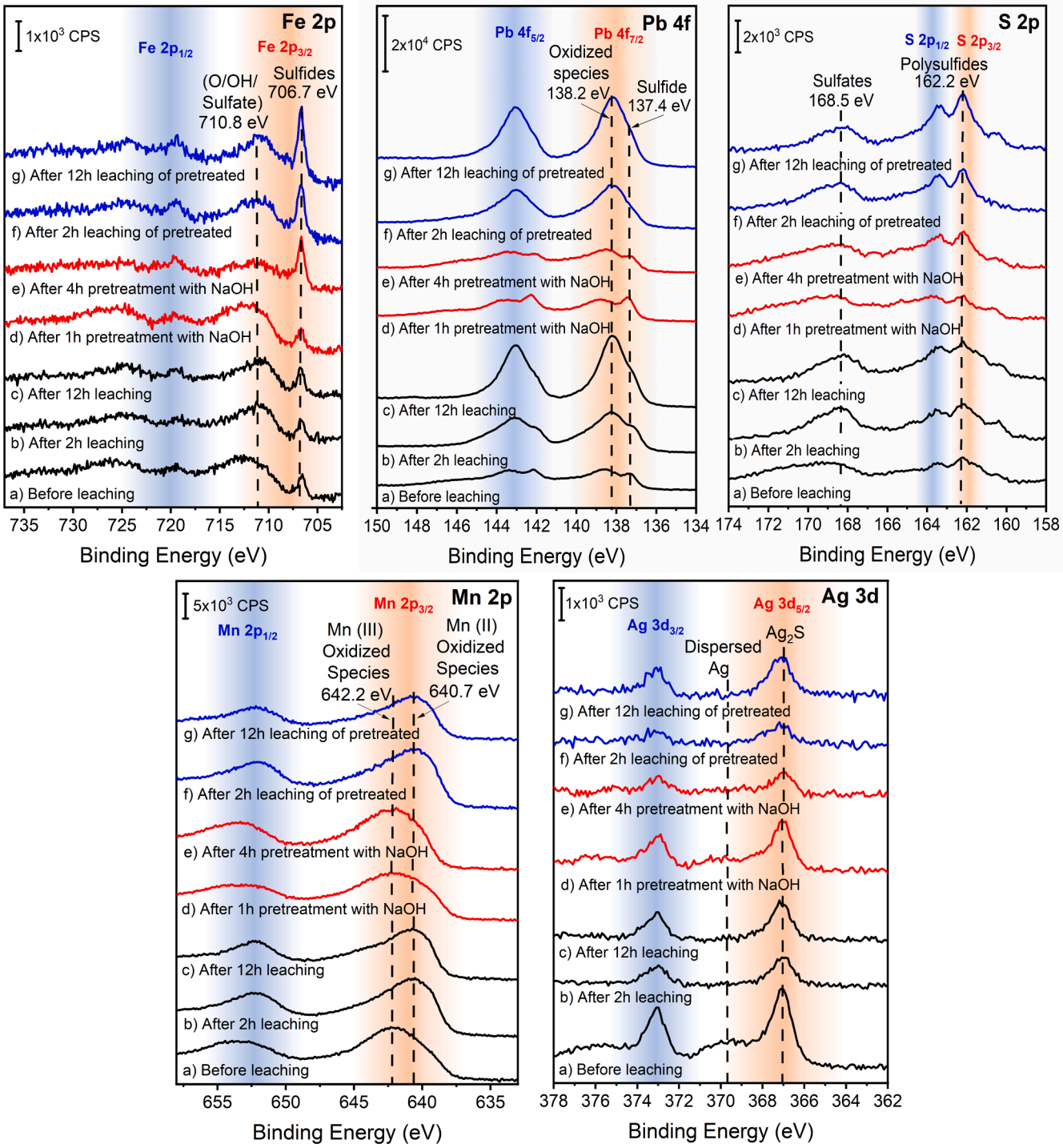

Fig. 3. Surface changes during conventional leaching and leaching after an alkaline pretreatment of a polymetallic (Fe-Pb-Mn) sulfide at times 0, 2 and 12 h. Fe 2p region, Pb 4f region, S 2p region (with spin–orbit coupling marked only for polysulfides), Mn 2p region, and Ag 3d region. For each panel representing an element, spectra correspond to a) Initial sample, b) After leaching for 2 h, c) After leaching for 12 h, d) After alkaline pretreatment for 1 h, e) After alkaline pretreatment for 4 h, f) After 2 h of leaching of the pretreated sample, g) After 12 h of leaching of the pretreated sample.

manganese, lead, and silver were either not detected in solution or detected in negligible amounts. XPS will be used to complement this information by following the changes at the surface level during the alkaline pretreatment. The S 2p region in Fig. 3 shows that the sulfur species are better defined after the pretreatment, likely because oxidized and neutral species (elemental S) have been removed and/or dissolved. Interestingly, the Fe 2p region shows a more intense signal for iron sulfide (706.7 eV), confirming that sulfide species are now dominant on the pretreated surface. No significant changes are observed in the Pb 4f and Mn 2p spectral regions. The signal corresponding to silver decreases in intensity, but since the pretreatment does not appear to dissolve silver, this change is likely due to the formation of surface layers over silver-containing minerals.

The leaching of pretreated samples is also followed by XPS. Perhaps the most remarkable change is the fact that the Fe 2p signal shows a higher intensity for the disulfide (pyrite) signal at 706.7 eV. This

Table 4
Average surface composition (At%) of Fe, Pb, S, Ag, and Mn in (Fe-Pb-Mn) sulfide ore samples before hydrometallurgical pretreatments, during conventional leaching, during alkaline pretreatment and during cyanidation following the pretreatment. Data are based on the XPS survey spectra collected in triplicates for each element.

Spectra	Fe	Pb	S	Ag	Mn
Conventional leaching					
Before leaching	9.6 ± 0.5%	14.1 ± 1.4%	43.4 ± 0.6%	2.6 ± 0.4%	30.3 ± 0.9%
After 2 h leaching	6.8 ± 0.3%	15.6 ± 0.7%	49.6 ± 1.2%	0.8 ± 0.2%	27.3 ± 1.9%
After 12 h leaching	6.8 ± 0.1%	18.9 ± 1.5%	48.8 ± 0.8%	0.7 ± 0.1%	24.9 ± 1.7%
Leaching with NaOH pretreatment					
Before pretreatment	9.6 ± 0.5%	14.1 ± 1.4%	43.4 ± 0.6%	2.6 ± 0.4%	30.3 ± 0.9%
After 1 h pretreatment with NaOH	10.5 ± 0.3%	13.5 ± 0.9%	41.9 ± 0.4%	1.6 ± 0.2%	32.6 ± 1.7%
After 4 h pretreatment with NaOH	9.9 ± 0.1%	11.6 ± 0.5%	45.6 ± 0.7%	0.8 ± 0.1%	32.3 ± 1.3%
After 2 h leaching	8.0 ± 0.2%	17.7 ± 0.8%	40.9 ± 0.8%	0.7 ± 0.2%	32.7 ± 0.8%
After 12 h leaching	8.2 ± 0.2%	19.1 ± 0.4%	47.5 ± 0.6%	0.7 ± 0.1%	24.4 ± 0.6%

indicates that the pretreatment exposes fresh pyrite surfaces and that these surfaces are not oxidized or covered during cyanide leaching. It is possible that this is due to the alkaline pretreatment removing species which would otherwise cover the pyrite surfaces. Supporting the hypothesis that fresh sulfide surfaces are maintained during leaching of the pretreated samples, the sulfur region shows sharp, well-defined peaks corresponding to sulfides and polysulfides.

The behavior of lead during cyanide leaching is the same regardless of whether the ore underwent an alkaline pretreatment or not. In both cases, cyanidation starts with both lead sulfide (galena) and oxidized lead species. During the leaching process, the oxidized species become more prominent, and the signal of lead increases its intensity. The increase in surface-level lead content is likely associated with lead re-adsorption over the surface of the pretreated ore during leaching. The behavior of manganese is also similar for the leaching of both untreated and pretreated ores. This is expected as the pretreatment did not appear to cause oxidation state changes for manganese. However, it is worth noting that the elemental concentration of surface-level manganese during leaching after the pretreatment is very different from the results of leaching of the untreated ore. The surface concentration of manganese (Table 4) decreases sharply after leaching the pretreated ore, which can be explained by the continuous dissolution of manganese, during a period in which the elemental composition of sulfur increases dramatically, while lead content continues increasing as well.

4. Conclusions

Based on the observations described above, a summary of the observed phenomena for conventional leaching and leaching after alkaline pretreatment for a polymetallic sulfide ore is provided:

(A) Conventional leaching
- Total Ag extraction reaches ~ 40%, consuming ~ 50 kg NaCN/t of ore.
- Pyrite is not oxidized during leaching.
- Removal of Pb from within the ore, followed by its build-up on the surface (re-adsorption).
- Mn (III) is reduced to Mn (II), at least at surface level.
- Oxidized silver, iron, and manganese species are dissolved.

(B) Leaching after alkaline pretreatment
- Total Ag extraction reaches ~ 80%, consuming ~ 30 kg NaCN/t of ore.
- Pretreatment exposes fresh pyrite surfaces.
- Pretreatment removes elemental sulfur at bulk level; other oxidized sulfur-containing species are also removed or covered-up.
- Pretreatment does not remove a significant amount of silver.
- Removal of Pb from within the ore, followed by its build-up on the surface (re-adsorption).
- Mn (III) is reduced to Mn (II), at least at surface level.
- Oxidized silver, iron, and manganese species are dissolved.

The effect of an alkaline pretreatment before cyanidation on a polymetallic (Pb-Mn-Fe) sulfide ore containing silver was investigated. It was found that the pretreatment dissolved sulfur species (mainly elemental sulfur) and exposed fresh sulfide surfaces. These changes lead to a simultaneous increase in silver extraction and to a decrease in cyanide consumption. It was also identified that the leaching process promotes the dissolution and readsorption of lead, but this process is observed to occur in both the untreated and the pretreated samples. A more detailed mineralogical study of the sample before and over the course of the assessed hydrometallurgical processes is required to understand their effect on the ore at a mineral scale.

CRediT authorship contribution statement

Gonzalo Larrabure: Formal analysis, Data curation, Writing – original draft, Writing – review & editing, Visualization. **Dhamelyz Silva-Quiñones:** Formal analysis, Data curation, Writing – review & editing, Visualization. **Andrew V. Teplyakov:** Conceptualization, Validation, Formal analysis, Resources, Writing – review & editing, Supervision. **Juan Carlos F. Rodriguez-Reyes:** Conceptualization, Methodology, Validation, Formal analysis, Resources, Writing – review & editing, Supervision, Project administration, Funding acquisition.

Declaration of Competing Interest

The authors declare that they have no known competing financial interests or personal relationships that could have appeared to influence the work reported in this paper.

Data availability

Data will be made available on request.

Acknowledgements

This research was possible through the support of ProCiencia – CONCYTEC and the World Bank (Contracts 002-2016 and 106-2018). The authors would like to thank the valuable work of Alejandro Alarcon, Carlos Segura, Carlos Gamarra (UTEC), Mackenzie Williams and Fei Gao (UD) in data collection. The authors would like to acknowledge the United States National Science Foundation (US NSF) for the support of summer research experience for undergraduates at the University of Delaware as a part of the CMMI2035154 grant. The participation of GL was possible through the Real Life Experience (RLE) program and through the Provost Scholarship, both at UTEC. Karinna Visurraga is thanked for administrative support.

Appendix A. Supplementary data

Supplementary data to this article can be found online at https://doi.org/10.1016/j.mineng.2023.108325.

References

Abdel-Samad, H., Watson, P.R., 1998. An XPS study of the adsorption of lead on goethite (FeOOH). Applied Surface Science 46–54. https://doi.org/10.1016/S0169-4332(98)00337-7.

Alarcón, A., Segura, C., Gamarra, C., Rodriguez-Reyes, J.C.F., 2018. Green chemistry in mineral processing: Chemical and physical methods to enhance the leaching of silver and the efficiency in cyanide consumption. Pure and Applied Chemistry 90, 1109–1120. https://doi.org/10.1515/pac-2017-0904.

Anderson, C.G., 2016. Alkaline sulfide gold leaching kinetics. Minerals Engineering 92, 248–256. https://doi.org/10.1016/j.mineng.2016.01.009.

Ansari, J.R., Singh, N., Mohapatra, S., Ahmad, R., Saha, N.R., Chattopadhyay, D., Mukherjee, M., Datta, A., 2019. Enhanced near infrared luminescence in Ag@Ag2S core-shell nanoparticles. Applied Surface Science 463, 573–580. https://doi.org/10.1016/j.apsusc.2018.08.244.

Arslan, F., Ozdamar, D., Muduroglu, M., 2003. Cyanidation of Turkish gold-silver ore and the use of hydrogen peroxide. European Journal of Mineral Processing and Environmental Protection 3, 309–315.

Aylmore, M.G., 2001. Treatment of a refractory gold-copper sulfide concentrate by copper ammoniacal thiosulfate leaching. Minerals Engineering 14, 615–637. https://doi.org/10.1016/S0892-6875(01)00057-7.

Bas, A.D., Koc, E., Yazici, Y.E., Deveci, H., 2015. Treatment of copper-rich gold ore by cyanide leaching, ammonia pretreatment and ammoniacal cyanide leaching. Transactions of the Nonferrous Metals Society of China 25, 597–607. https://doi.org/10.1016/S1003-6326(15)63642-1.

Bas, A.D., Larachi, F., Laflamme, P., 2018. The effect of pyrite particle size on the electrochemical dissolution of gold during cyanidation. Hydrometallurgy 175, 367–375. https://doi.org/10.1016/j.hydromet.2017.12.016.

Bastl, Z., Baláz, P., 1993. X-ray photoelectron spectroscopy study of galena dissolution in ferric chloride media. Journal of Materials Science Letters 12, 789–790.

Birich, A., Stopic, S., Friedrich, B., 2019. Kinetic investigation and dissolution behavior of cyanide alternative gold leaching reagents. Scientific Reports 9, 1–10. https://doi.org/10.1038/s41598-019-43383-4.

Calderon, V.S., Galindo, R.E., Benito, N., Palacio, C., Cavaleiro, A., Carvalho, S., 2013. Ag + release inhibition from ZrCN-Ag coatings by surface agglomeration mechanism: Structural characterization. Journal of Physics D: Applied Physics 46. https://doi.org/10.1088/0022-3727/46/32/325303.

Carver, J.C., Schweitzer, G.K., Carlson, T.A., 1972. Use of XRay photoelectron spectroscopy to study bonding in Cr, Mn, Fe, and Co compounds. The Journal of Chemical Physics 973. https://doi.org/10.1063/1.1678348.

Celep, O., Alp, I., Deveci, H., Vicil, M., 2009. Characterization of refractory behaviour of complex gold/silver ore by diagnostic leaching. Transactions of the Nonferrous Metals Society of China 19, 707–713. https://doi.org/10.1016/S1003-6326(08)60337-4.

Celep, O., Alp, I., Deveci, H., 2011. Improved gold and silver extraction from a refractory antimony ore by pretreatment with alkaline sulphide leach. Hydrometallurgy 105, 234–239. https://doi.org/10.1016/j.hydromet.2010.10.005.

Celep, O., Bas, A.D., Yazici, E.Y., Alp, I., Deveci, H., 2014. Improvement of silver extraction by ultra-fine grinding prior to cyanide leaching of the plant tailings of a refractory silver ore. Mineral Processing and Extractive Metallurgy Review 36, 1–39. https://doi.org/10.1080/08827508.2014.928621.

Celep, O., Yazici, E.Y., Altinkaya, P., Deveci, H., 2019. Characterization of a refractory arsenical silver ore by mineral liberation analysis (MLA) and diagnostic leaching. Hydrometallurgy 189, 105106. https://doi.org/10.1016/j.hydromet.2019.105106.

Ciftci, H., Akcil, A., 2010. Effect of biooxidation conditions on cyanide consumption and gold recovery from a refractory gold concentrate. Hydrometallurgy 104, 142–149. https://doi.org/10.1016/j.hydromet.2010.05.010.

Dai, X., Simons, A., Breuer, P., 2012. A review of copper cyanide recovery technologies for the cyanidation of copper containing gold ores. Minerals Engineering 25, 1–13. https://doi.org/10.1016/j.mineng.2011.10.002.

De Caro, T., Riccucci, C., Parisi, E.I., Caschera, D., Faraldi, F., 2013. Ancient silver extraction in the montevecchio mine basin (Sardinia, Italy): Micro-chemical study of pyrometallurgical materials. Applied Physics A 945–957. https://doi.org/10.1007/s00339-013-7722-3.

Derycke, V., Kongolo, M., Benzaazoua, M., Mallet, M., Barrès, O., Donato, P.D., Bussière, B., Mermillod-Blondin, R., 2013. Surface chemical characterization of different pyrite size fractions for flotation purposes. International Journal of Mineral Processing 118, 1–14. https://doi.org/10.1016/j.minpro.2012.10.004.

Deschênes, G., Lastra, R., Brown, J.R., Jin, S., May, O., Ghali, E., 2000. Effect of lead nitrate on cyanidation of gold ores: Progress on the study of the mechanisms. Minerals Engineering 13, 1263–1279. https://doi.org/10.1016/S0892-6875(00)00109-6.

Deschênes, G., Rajala, J., Pratt, A., Guo, H., Fulton, M., Mortazavi, S., 2011. Advances in the cyanidation of silver. Soc. Mining Metall. Explor. 28, 37–43. https://doi.org/10.1007/BF03402323.

Duan, Y., Rani, S., Zhang, Y., Ni, C., Newberg, J.T., Teplyakov, A.V., 2017. Silver deposition onto modified silicon substrates. Journal of Physical Chemistry C 121, 7240–7247. https://doi.org/10.1021/acs.jpcc.6b12896.

Duan, Y., Rani, S., Newberg, J.T., Teplyakov, A.V., 2018. Investigation of the influence of oxygen plasma on supported silver nanoparticles. J. Vac. Sci. Technol. A Vacuum, Surfaces, Film. 36, 01B101. https://doi.org/10.1116/1.4986208.

Ellis, S., Senanayake, G., 2004. The effects of dissolved oxygen and cyanide dosage on gold extraction from a pyrrhotite-rich ore. Hydrometallurgy 72, 39–50. https://doi.org/10.1016/S0304-386X(03)00131-2.

Fantauzzi, M., Elsener, B., Atzei, D., Rigoldi, A., Rossi, A., 2015. Exploiting XPS for the identification of sulfides and polysulfides. R. Soc. Chem. 75953–75963. https://doi.org/10.1039/C5RA14915K.

Fleming, C.A., 1992. Hydrometallurgy of precious metals recovery. Hydrometallurgy 30, 127–162. https://doi.org/10.1016/0304-386X(92)90081-A.

Fraser, K.S., Walton, R.H., Wells, J.A., 1991. Processing of refractory gold ores. Minerals Engineering 4, 1029–1041. https://doi.org/10.1016/0892-6875(91)90081-6.

Godociková, E., Baláz, P., Bastl, Z., Brabec, L., 2002. Spectroscopic study of the surface oxidation of mechanically activated sulphides. Applied Surface Science 200, 36–47. https://doi.org/10.1016/S0169-4332(02)00609-8.

Graham, A.M., Bouwer, E.J., 2012. Oxidative dissolution of pyrite surfaces by hexavalent chromium: Surface site saturation and surface renewal. Geochimica et Cosmochimica Acta 83, 379–396. https://doi.org/10.1016/j.gca.2012.01.006.

Herbert Jr, R.B., Pratt, A.R., Blowes, D.W., Benner, S.G., 1997. Surface oxidation of iron monosulphide: An X-ray photoelectron spectroscopic study. Mineralogical Magazine 62, 1997–1998.

Hobson, E.L., Wincott, P., Vaughan, D.J., Pattrick, R.A.D., 2006. An investigation of extreme silver enrichment at tennantite surfaces exposed to alkaline solutions: An XPS-based study. Mineralogical Magazine 70, 445–457. https://doi.org/10.1180/0026461067040345.

Jeffrey, M.I., Ritchie, I.M., 2000. The leaching of gold in cyanide solutions in the presence of impurities II. The effect of silver. Journal of the Electrochemical Society 147, 3272–3276. https://doi.org/10.1149/1.1393894.

Jones, L., Hackl, R.P., 1999. Sources of high cyanide consumption for a biooxidized refractory gold concentrate. Process Metall. 9, 337–346. https://doi.org/10.1016/S1572-4409(99)80034-0.

Kartio, I., Wittstock, G., Laajalehto, K., Hirsch, D., Simola, J., Laiho, T., Szargan, R., Suoninen, E., 1997. Detection of elemental sulphur on galena oxidized in acidic solution. International Journal of Mineral Processing 51, 293–301. https://doi.org/10.1016/s0301-7516(97)00028-8.

Kaspar, T.C., Droubay, T., Chambers, S.A., Bagus, P.S., 2010. Spectroscopic evidence for Ag(III) in highly oxidized silver films by X-ray photoelectron spectroscopy. Journal of Physical Chemistry C 114, 21562–21571. https://doi.org/10.1021/jp107914e.

Khalid, M., Larachi, F., 2016. Effect of silver on gold cyanidation in mixed and segregated sulphidic minerals. Canadian Journal of Chemical Engineering 9999, 1–10. https://doi.org/10.1002/cjce.22705.

Khoshkhoo, M., Dopson, M., Shchukarev, A., Sandström, Å., 2014. Chalcopyrite leaching and bioleaching: An X-ray photoelectron spectroscopic (XPS) investigation on the nature of hindered dissolution. Hydrometallurgy 149, 220–227. https://doi.org/10.1016/j.hydromet.2014.08.012.

Kianinia, Y., Khalesi, M.R., Abdollahy, M., Hefter, G., Senanayake, G., Hnedkovsky, L., Darban, A.K., Shahbazi, M., 2018. Predicting cyanide consumption in gold leaching: A kinetic and thermodynamic modeling approach. Minerals 8, 1–13. https://doi.org/10.3390/min8030110.

Kyle, J.H., 1997. Stability of metal cyanide and hydroxide complexes, in: World Gold '97. Singapore.

La Brooy, S.R., Linge, H.G., Walker, G.S., 1994. Review of gold extraction from ores. Miner. Eng. 7, 1213–1241. https://doi.org/10.1016/0892-6875(94)90114-7.

Larrabure, G., Chero-Osorio, S., Silva-Quiñones, D., Benndorf, C., Williams, M., Gao, F., Gamarra, C., Alarcón, A., Segura, C., Teplyakov, A., Rodriguez-Reyes, J.C.F., 2021. Surface processes at a polymetallic (Mn-Fe-Pb) sulfide subject to cyanide leaching under sonication conditions and with an alkaline pretreatment: Understanding differences in silver extraction with X-ray photoelectron spectroscopy (XPS). Hydrometallurgy 200. https://doi.org/10.1016/j.hydromet.2020.105544.

Larrabure, G., Rodríguez-Reyes, J.C.F., 2021. A review on the negative impact of different elements during cyanidation of gold and silver from refractory ores and strategies to optimize the leaching process. Minerals Engineering 173. https://doi.org/10.1016/j.mineng.2021.107194.

Lottermoser, B., 2003. Cyanidation wastes of gold-silver ores. Mine Wastes. 171–187. https://doi.org/10.1007/978-3-662-05133-7_5.

Marabini, A.M., Contini, G., Cozza, C., 1993. Review: Surface spectroscopic techniques applied to the study of mineral processing. International Journal of Mineral Processing 38, 1–20. https://doi.org/10.1016/0301-7516(93)90062-F.

Mikali, M., Barbouchi, A., Idouhli, R., Abouelfida, A., Yaacoubi, A., Benzakour, I., Faqir, H., Boulaamail, A., Bacaoui, A., 2023. Electrochemical behavior of silver during cyanidation in the presence of sulfide minerals. Chemical Papers 77, 2103–2113. https://doi.org/10.1007/s11696-022-02613-2.

Mills, P., Sullivan, J., 1983. A study of the core level electrons in iron and its three oxides by means of x-ray photoelectron spectroscopy. Journal of Physics D: Applied Physics 723. https://doi.org/10.1088/0022-3727/16/5/005.

Moulder, J.F., Stickle, W.F., Sobol, P.E., Bomben, K.D., 1992. Handbook of X-ray Photoelectron Spectroscopy. Perkin-Elmer Corporation, Minnesota.

Nunan, T.O., Viana, I.L., Peixoto, G.C., Ernesto, H., Verster, D.M., Pereira, J.H., Bonfatti, J.M., Cesar Teixeira, L.A., 2017. Improvements in gold ore cyanidation by pre-oxidation with hydrogen peroxide. Minerals Engineering 108, 67–70. https://doi.org/10.1016/j.mineng.2017.01.006.

Oku, M., Hirokawa, K., 1976. X-ray photoelectron spectroscopy of Co3O4, Fe3O4, Mn3O4 and related compounds. J. Electron Spectros. Relat. Phenomena 8, 475–481. https://doi.org/10.1016/0368-2048(76)80034-5.

Parker, A., Klauber, C., Kougianos, A., Watling, H.R., Van Bronswijk, W., 2003. An X-ray photoelectron spectroscopy study of the mechanism of oxidative dissolution of chalcopyrite. Hydrometallurgy 71, 265–276. https://doi.org/10.1016/S0304-386X(03)00165-8.

Portilla, R.E., He, C., Jacome-Collazos, M., Visurraga, K., Chirif, H., Teplyakov, A.V., Rodríguez-Reyes, J.C.F., 2020. Acidic pretreatment of a copper-silver ore and its

beneficial effect on cyanide leaching. Minerals Engineering 149. https://doi.org/10.1016/j.mineng.2020.106233.
Rees, K.L., Van Deventer, J.S.J., 2000. Preg-robbing phenomena in the cyanidation of sulphide gold ores. Hydrometallurgy 58, 61–80. https://doi.org/10.1016/S0304-386X(00)00131-6.
Salas-Martell, D., Pareja-Guzman, G., Tello-Hijar, J., Rodriguez-Reyes, J.C.F., 2020. Leaching of a pyrite-based ore containing copper using sulfuric acid and hydrogen peroxide. Int. J. Ind. Chem. 11 https://doi.org/10.1007/s40090-020-00212-2.
Schweitzer, G.K., Pesterfield, L.L., 2010. The Aqueous Chemistry of The Elements, Journal of Chemical Information and Modeling. Oxford University Press, New York.
Senanayake, G., 2008. A review of effects of silver, lead, sulfide and carbonaceous matter on gold cyanidation and mechanistic interpretation. Hydrometallurgy 90, 46–73. https://doi.org/10.1016/j.hydromet.2007.09.013.
Silva-Quiñones, D., He, C., Jacome-Collazos, M., Benndorf, C., Teplyakov, A.V., Rodriguez-Reyes, J.C.F., 2018. Identification of surface processes in individual minerals of a complex ore through the analysis of polished sections using polarization microscopy and X-ray photoelectron spectroscopy (XPS). Minerals 1–9. https://doi.org/10.3390/min8100427.
Tiwari, P., Malik, G., Chandra, R., 2018. Phase-dependent structural and electrochemical properties of single crystalline MnS thin films deposited by DC reactive sputtering. Journal of Applied Physics 195106. https://doi.org/10.1063/1.5053875.
Tremolada, J., Dzioba, R., Bernardo-Sánchez, A., Menéndez-Aguado, J.M., 2010. The preg-robbing of gold and silver by clays during cyanidation under agitation and heap leaching conditions. International Journal of Mineral Processing 94, 67–71. https://doi.org/10.1016/j.minpro.2009.12.001.
Umezawa, Y., Reilley, C.N., 1978. Effect of argon ion bombardment on metal complexes and oxides studied by X-ray photoelectron spectroscopy. Analytical Chemistry 50, 1290–1295. https://doi.org/10.1021/ac50031a025.
Wan, M., Shchukarev, A., Lohmayer, R., Planer-Friedrich, B., Peiffer, S., 2014. Occurrence of surface polysulfides during the interaction between ferric (Hydr) Oxides and aqueous sulfide. Environmental Science & Technology 48, 5076–5084. https://doi.org/10.1021/es405612f.
Yin, Q., Vaughan, D.J., England, K.E.R., Kelsall, G.H., Brandon, N.P., 2000. Surface oxidation of chalcopyrite (CuFeS2) in alkaline solutions. Jounal Electrochem. Soc. 147, 2945–2951. https://doi.org/10.1149/1.1393629.
Zia, Y., Mohammadnejad, S., Abdollahy, M., 2019. Gold passivation by sulfur species: A molecular picture. Minerals Engineering 134, 215–221. https://doi.org/10.1016/j.mineng.2019.02.009.
Zia, Y., Mohammadnejad, S., Abdollahy, M., 2020. Destabilisation of gold cyanide complex by sulphur species: A computational perspective. Hydrometallurgy 197. https://doi.org/10.1016/j.hydromet.2020.105459.